Journal of Materials Chemistry A

Accepted Manuscript

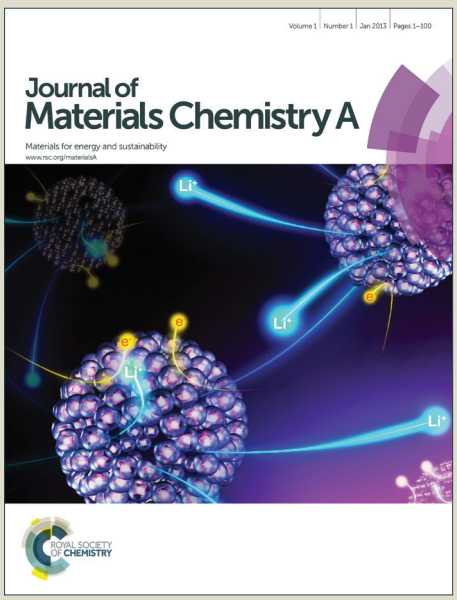

ROYAL SOCIETY OF CHEMISTRY

www.rsc.org/materialsA

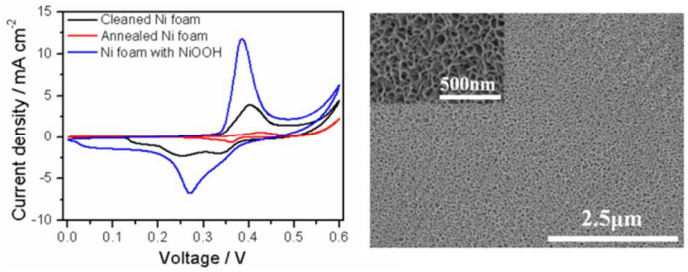

Porous Nickel Oxide-Hydroxide are deposited on passivated 3D nickel foam by anodic electrodeposition for high performance supercapacitor electrode.

Cite this: DOI: 10.1039/c0xx00000x

www.rsc.org/xxxxxx

ARTICLE TYPE

Anodic Electrodeposition of Porous Nickel Oxide-Hydroxide Film on Passivated Nickel Foam for Supercapacitors

Lin Gu [a], Yewu Wang [a*], Ren Lu [a], Liao Guan [a], Xinsheng Peng [b], and Jian Sha [a*]

Received (in XXX, XXX) Xth XXXXXXXXX 20XX, Accepted Xth XXXXXXXXX 20XX

DOI: 10.1039/b000000x

The response current of Ni foam in alkaline solutions can be reduced significantly by high-temperature annealing, making it more suitable for current collectors, and porous NiO(OH) film deposited on the passivated 3D Ni foam by anodic electrodeposition shows a ultrahigh specific capacitance of 2302 F g^{-1} at 1 A g^{-1}.

Supercapacitors (SCs), with high power densities (>10 kW kg^{-1}) and long cycle lives (>10^6 cycles),[1-3] are a new type of energy-storage device. According to the energy storage mechanisms, supercapacitors are divided into electrical double-layer capacitors (EDLCs) and pseudocapacitors. Carbon materials, such as activated carbons, aerogels and nanostructures, have been used as active materials for EDLCs,[4,5] in which only adsorption and desorption of electrolyte ions on electrode materials occur during the charge/discharge process. For pseudocapacitors, reversible redox reactions occur during cycling process. The active material, metal oxides and conducting polymers, have been widely studies.[6,7]

Nickel oxide (NiO) and nickel hydroxide ($Ni(OH)_2$) are potential candidates for supercapacitors because of the high theoretical capacitance (2573 F g^{-1} for NiO and 2073 F g^{-1} for $Ni(OH)_2$),[8,9] low cost and low environmental impact. Nickel oxide with different morphologies, such as porous thin-film,[10] porous nano-sheets,[11] three-dimensional nanonetwork,[12] porous hollow spheres,[13] hollow nanofibers,[14] nanotubes[15] and nanorod arrays,[16] fabricated by chemical precipitation methods have been reported recently and specific capacitances of 130 ~ 2018 F g^{-1} are achieved. Electrochemical preparation of nickel oxide/hydroxide can be divided into two methods: cathodic deposition and anodic deposition.[17] Cathodic electrodeposition is normally performed in nickel nitrate solution, in which nitrate is reduced to ammonia and OH- ions. The nickel ions then react with OH^- ions to form insoluble nickel hydroxides. With proper annealing, $Ni(OH)_2$[18,19] and NiO[20,21] can be achieved. During anodic electrodeposition, Ni^{2+} ions are oxidized to Ni^{3+} ions in the solution consisted of sodium acetate, nickel sulfate and sodium sulfate. Then Ni^{3+} ions react with OH^- ions to form insoluble nickel oxide-hydroxide (NiO(OH)).[17,22-24] Compared with the NiO or $Ni(OH)_2$ nanoparticles achieved by cathodic deposition, nickel oxide/hydroxides thin films prepared by anodic deposition are porous.

Nickel foam is widely used as the current collector in supercapacitors because of its three dimensional structure and excellent conductivity. NiO and $Ni(OH)_2$ also can be directly deposited on Ni foam by electrochemical methods and no binder is needed. Moreover, compared with normal chemical precipitation methods, the mass loading can be easily controlled by simply adjusting the electrodeposition parameters. $Ni(OH)_2$[18] and NiO[20] nanostructures deposited on 3D Ni foam not only facilitate the penetration of electrolyte into the whole electrode, but also shorten the ions diffusion distance, hence this structure shows remarkable supercapacitor performance. However, actually, nickel foam in alkaline solutions also makes contribution to the measured capacitance due to its active surface, and the calculated specific capacitance would be higher than the real capacitance of the active materials especially when the quantity of active materials is small. Currently, electrochemically inert current collectors, such as Ti or Pt foil have been suggested to replace the Ni foam in supercapacitors.[25] But Ti or Pt foils do not have 3D structure, moreover, they are much more expensive than Ni foam. In this paper, we introduce an effective method to passivate the active surface of nickel foam to decrease the contribution of Ni foam to the calculated capacitance. The passivation mechanism is also proposed in the paper. Then, porous nickel oxide-hydroxide materials are deposited directly on the passivated Ni foam by anodic electrodeposition and this electrode shows excellent electrochemical performance.

Nickel foams were used as the current collector, and cleaned with acetone and deionized water in an ultrasound bath for 5 min, respectively. Subsequently, they were sonicated in 4 M HCl solution for 10 min, and then washed with deionized water and absolute ethanol, and dried in air. The cleaned nickel foams were annealed in a furnace tube (with the pressure of 6 Pa) at 1000 °C for 2 hours to passivate the surface. Nickel oxide-hydroxide was deposited on the nickel foams by anodic electrodeposition with the current density of 1 mA cm^{-2} for 1 hour in a solution of 0.13 M sodium acetate, 0.13 M nickel sulfate and 0.1 M sodium sulfate at room temperature. After deposition, the samples were rinsed with deionized water and annealed for 1 h at 200 °C in air. The mass of the active material was got by weighing the nickel foam before and after deposition of NiO(OH), and the mass is calculated to be 0.25 mg cm^{-2}.

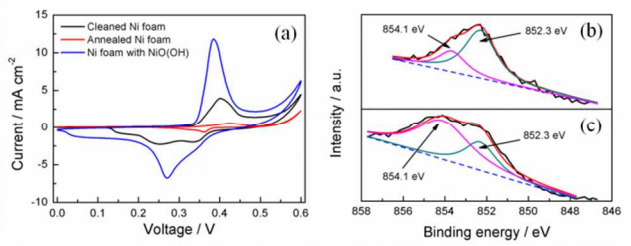

Fig. 1 (a) CV curves (with the scan rate of 5 mV s^{-1}) of the cleaned Ni foam (black curve), the annealed Ni foam (red curve) and the annealed Ni foam deposited with NiO(OH) (blue curve); (b) XPS spectra of the Ni ($2p_{3/2}$) of the cleaned Ni foam; (c) XPS spectra of the Ni ($2p_{3/2}$) of the annealed Ni foam.

Morphology of the nickel oxide/hydroxide was investigated by scanning electron microscopy (SEM) (CorlzeisD, Utral 55). Microstructure of NiO(OH) nanostructure and their EDS analysis were carried out by transmission electron microscopy (TEM) (JEM-2010(HR)/200KV). The X-ray photoelectron spectroscopy (XPS) measurements were performed on VG ESCALAB MARK II device with Mg-Kα (hν = 1253.6 eV) excitation source. The electrochemical performance was characterized in a three-electrode system with 1 M KOH solution as electrolyte. Cyclic voltammetry (CV) and galvanostatic charge–discharge (GV) were tested by CHI 660D electrochemical station with a platinum foil as counter electrode and a saturated Ag/AgCl as reference electrode.

Fig. 1(a) shows the CV curves (at the scan rate of 5 mV s^{-1}) of the as-cleaned Ni foam (black curve), the annealed Ni foam (red curve) and the annealed-Ni foam deposited with nickel oxide-hydroxide (blue curve). It is obvious that, after annealing, the response current of the Ni foam is much weaker than that of the as-cleaned foam. The calculated capacitance per projected area of the annealed Ni foam is only 18.2 mF cm^{-2}, which is much smaller than that of the as-cleaned foam (145.6 mF cm^{-2}). The existence of nickel hydroxide or nickel oxide on the surface of the as-cleaned Ni foam contributes to the capacitance.[25] Although the cleaning process in HCl solution is to remove the native nickel oxide on the surface of nickel foams, hydrochloric acid may also react with nickel foams and makes their surfaces more rough and chemical active. Fortunately, the active surface of Ni foams can be "passivated" effectively by high temperature annealing. To explore what happened after the passivation, XPS analysis has been performed on the cleaned Ni foam and the annealed Ni foam without inserting in KOH solution, and the results are shown in Fig. 1(b) and (c). The Ni ($2p_{3/2}$) of the cleaned nickel foam can be deconvolved into two peaks at 854.1 and 852.3 eV, corresponding to nickel Ni^{2+} in NiO and nickel metal.[25] Figs. 1(b) and (c) obviously show that, after annealing, the peak at 854.1 eV strengthens compared with the cleaned Ni foam, meaning that there are more nickel oxide forming on the surface of the foam. During the high temperature annealing, the residual oxygen reacted with the nickel foam to form a thin film of nickel oxide on the surface. The physical and chemical characteristics of the nickel oxide changes with annealing temperatures, especially when the temperature approaches 1000 °C, have been reported.[26,27] With the annealing temperature increasing, the crystalline-phase of the nickel oxide becomes

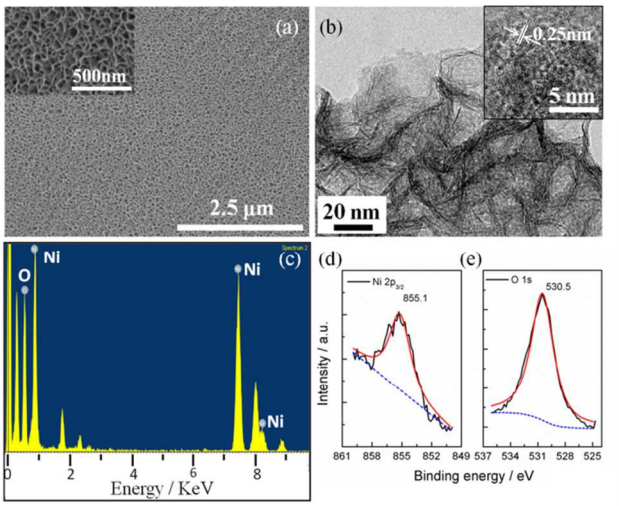

Fig. 2 (a) SEM images of the nickel oxide-hydroxide on nickel foam; (b) Low-magnification and lattice-resolution TEM images of NiO(OH) thin film; (c) EDS spectrum taken on the NiO(OH) thin film; (d) and (e) XPS spectra of the Ni ($2p_{3/2}$) and O (1s) of the Ni foam deposited with nickel oxide-hydroxide.

better, and the density and resistivity increases, meanwhile, the solubility and chemical activity decreases. In our cases, after annealing, the compact nickel oxide on the foam surface protects the inner nickel from reacting with the electrolyte, resulting in the smaller response current.

Nickel oxide-hydroxide (NiO(OH)) was directly deposited on the annealed Ni foams by anodic electrodeposition. Fig. S4 shows the low magnification SEM image of NiO(OH) on Ni foam, which clearly reveals the uniformity of the NiO(OH). The high-magnification SEM images of Fig. 2(a) shows that the prepared nickel oxide-hydroxide is porous and composed of nanoflakes. To investigate the interior structures of NiO(OH), TEM analyses were also performed and the results are shown in Fig.2 (b). It can been seen from the low-magnification TME image that the NiO(OH) deposited on the Ni foam is a thin film with drapes, which is composed of interconnected nanoflakes. High-magnification TEM image shows some lattice fringe, meaning the nanostructure is polycrystalline. The lattice fringe spacing is measured to be 0.25 nm, the same as the interspacing of the (111) lattice planes of NiO(OH) (JCPDS 22-0444). EDS analysis in Fig. 2(c) shows signals of Ni and O and the other signals come from impurity and the TEM grid. Statistical analysis shows that the atomic ratio of Ni and O is about 0.5, consistent with chemical composition of NiO(OH). To further confirm the chemical composition, XPS analysis has been done and the results are shown in Fig. 2(d) and (e). The Ni ($2p_{3/2}$) peak at 855.1 eV and O (1s) peak at 530.5 eV correspond to the Ni^{2+} and O^{2-} in nickel oxide-hydroxide.[25]

The electrochemical performance of NiO(OH) on Ni foam is measured in 1 M KOH solution with the potential window of 0 ~ 0.6 V. CV curves of annealed Ni foam and annealed Ni foam with nickel oxide-hydroxide porous film are shown in Fig. 1(a). The response current of the annealed nickel foam is much weaker than that of the foam deposited with NiO(OH). The areal capacitance of the Ni foam deposited with NiO(OH) is 314.9 mF $cm^{-2,}$ while the areal capacitance of the Ni foam is only 18.2 mF

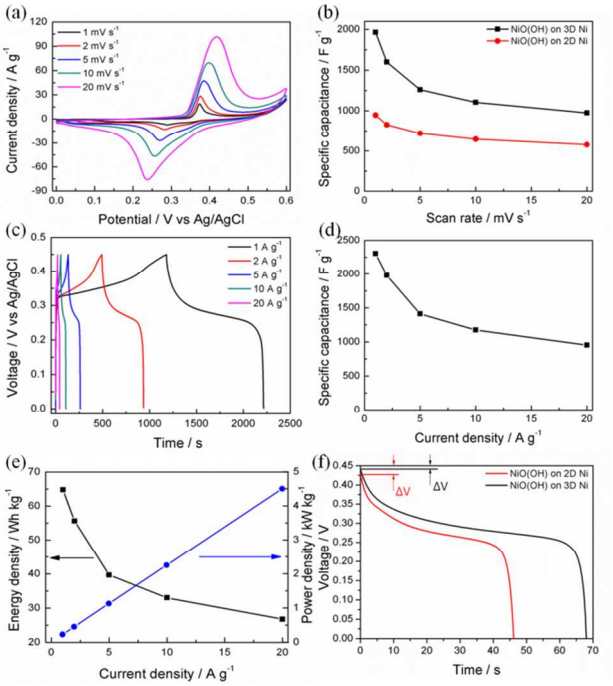

Fig. 3 (a) CV curves of NiO(OH) on passivated Ni foam at different scan rates (1~20 mV s^{-1}); (b) Specific capacitances of the nickel oxide-hydroxide on 3D nickel foam and 2D nickel plate as a function of scan rates (1-20 mV s^{-1}); (c) Charge-discharge curves of the nickel oxide-hydroxide on passivated Ni foam with different current densities (1~20 A g^{-1}); (d) Specific capacitances of the nickel oxide-hydroxide as a function of current densities (1-20 A g^{-1}); (e) Energy densities and power densities of the nickel oxide-hydroxide as a function of current densities.; (f) Galvanostatic discharge curves of the NiO(OH) on 3D and 2D nickel at the same current density (3mA cm^{-2}) and ΔV represents IR drops.

cm^{-2}. Such small contribution of the nickel foam to the total capacitance is almost negligible. CV curves of the NiO(OH) on Ni foam at different scan rates (1~20 mV s^{-1}) are shown in Fig. 3(a) and the calculated specific capacitances of NiO(OH) as a function of scan rates are shown in Fig. 3(b). The redox peaks are maintained at different scan rates and the shapes of these curves are similar, meaning that the capacitive behavior of the electrode is maintained over this range. The specific capacitance at the scan rate of 1 mV s^{-1} is 1964.4 F g^{-1} and the capacitance decreases with the increase of scan rate.

The electrochemical performance was also investigated by galvanostatic charge-discharge tests and the results are shown in Fig. 3(c). The potential window of 0 to 0.45 V is adopted in GV tests to avoid the apparent oxygen-evolution reaction. The specific capacitance of the NiO(OH) on 3D Ni foam calculated by GV curves is 2302 F g^{-1} at the current density of 1 A g^{-1}(Fig. 3(d)). This value is much higher than that of the nickel oxide/hydroxide deposited on plate electrodes by anodic electrodeposition method[17,22-24,28] and comparable to that of nickel oxide deposited on 3D nickel foam by the cathodic electrodeposition method.[20] The energy densities and power densities of NiO(OH) on Ni foam calculated from the GV tests are shown in Fig. 3(e) as a function of current densities. The highest energy density of 64.7 Wh kg^{-1} is got at the current

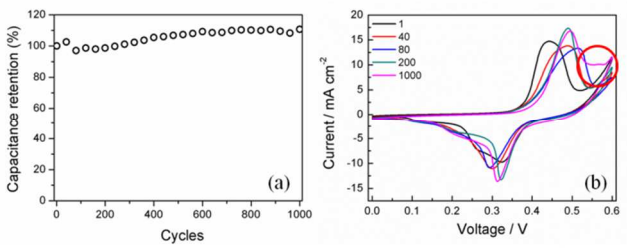

Fig. 4 (a) Cycling performance of the NiO(OH) on passivated Ni foam tested by cyclic voltammetry with the scan rate of 10 mV s^{-1}; (b) CV curves of the 1th,40th,80th,200th and 1000th cycle.

density of 1 A g^{-1} and the highest power density of 4.5 kW kg^{-1} is got at the current density of 20 A g^{-1}. Although the power density at 1 A g^{-1} is only 0.23 kW kg^{-1}, the energy density of 64.7 Wh kg^{-1} is one of the best results reported so far about nickel oxide/hydroxide supercapacitors.[11, 20, 29]

To explore the reason of the improved electrochemical performance of the NiO(OH) on 3D nickel foam, NiO(OH) was also deposited on 2D nickel plate with the same method, and the specific capacitances were shown in Fig. 3(b). It clearly shows that the specific capacitance of NiO(OH) on 2D nickel plate is much lower than that of NiO(OH) on 3D nickel foam. The galvanostatic discharge curves of the NiO(OH) on 3D and 2D nickel at the same current density are shown in Fig. 3(f). IR drops (ΔV) of the NiO(OH) on 3D and 2D nickel are 0.008 V and 0.021 V, respectively. This result indicates that the NiO(OH) on 3D nickel foam has lower internal resistance, which improves the transport and collection of electrons, resulting in the improved electrochemical performance.[31] The 3D structure of nickel foam, as well as the porous nanostructure of NiO(OH), facilitate the penetration of electrolyte into the whole electrode and shorten the ions diffusion distance in the active material, contributing to the high supercapacitor performance.[18,20,30]

Cycle stability is carried out by CV cycling at 10 mV s-1 and the result is shown in Fig. 4(a). The capacitance of NiO(OH) on Ni foam gradually increases to about 110% and keeps almost constant for 1000 cycles. CV curves at different cycles are shown in Fig. 4(b). In the first 100 cycles, the peak potential position changes a lot, which means the electrochemical performance are not very stable in the first few cycles. The initial process will activate the electrode.[11,32-34] After 200 cycles, the peak potential position changes very little and no other peaks were observed during the process as shown in CV curves of the 200th and 1000th cycle, meaning a stable electrochemical reversibility.[14,35] At higher positive potential, "Oxygen Evolution Reaction" happens and leads to the current increase, marked by the red circle in the figure.[36,37] From 200th to 1000th cycle, though the current signals related to the redox reactions of the active material changes very little, the current of the oxygen evolution reaction increases which contributes the calculated capacitance.

In summary, nickel oxide-hydroxide are deposited on the passivated 3D Ni foam by anodic electrodeposition and the supercapacitor electrode shows high specific capacitance, large energy density and long-term cyclic stability. High-temperature annealing passivates the surface of Ni foam and suppresses the reaction of Ni foam surface in KOH solution, making the Ni foam more suitable for current collectors in nickel oxide/hydroxide

supercapacitors. 3D structure of nickel foam and the nickel oxide-hydroxide nanostructure facilitate the penetration of electrolyte into the whole electrode and reduce the internal resistance, contributing to a high specific capacitance of 2302 F g^{-1} and a large energy density of 64.7 Wh kg^{-1} at the current density of 1 A g^{-1}. Also, the electrode shows good cyclic stability. Therefore, nickel oxide-hydroxide on passivated 3D Ni foam is promising for supercapacitor electrodes.

This work was supported by National Natural Science Foundation of China (No. 51272232), Program for New Century Excellent Talents in University, and the Fundamental Research Funds for the Central Universities.

Notes and references

[a] *Department of Physics & State Key Laboratory of Silicon Materials, Zhejiang University, Hangzhou, 310027, P. R. China. Emails: yewuwang@zju.edu.cn; phyjsha@zju.edu.cn; Fax:+86-571-87953746; Tel: +86-571-87953746.*

[b] *State Key Laboratory of Silicon Materials, Department of Materials Science and Engineering, Zhejiang University, Hangzhou, 310027, P. R. China.*

† Elecronic Supplementary Information (ESI) availabe: Experimental procedure, suporting figures.

1 D. H. Fritts, *J. Electrochem. Soc.*, 1997, **144**, 2233.
2 B. E. Conway, *J. Electrochem. Soc.*, 1991, **138**, 1539.
3 S. Sarangapani, B. V. Tilak and C. P. Chen, *J. Electrochem. Soc.*, 1996, **143**, 3791.
4 E. Frackowiak and F. Béguin, *Carbon*, 2001, **39**, 937.
5 A. G. Pandolfo and A. F. Hollenkamp, *J. Power Sources.*, 2006, **157**, 11.
6 N. L. Wu, *Mater. Chem. Phys.*, 2002, **75**, 6.
7 P. Simon and Y. Gogotsi, *Nat. Mater.*, 2008, **7**, 845.
8 X. Sun, G. K. Wang, J.-Y. Hwang and J. Lian, *J. Mater. Chem.*, 2011, **21**, 16581.
9 B. Gao, C.-Z. Yuan, L.-H. Su, L. Chen and X.-G Zhang, *J. Solid State Electrochem.*, 2009, **13**, 1251.
10 A.I. Inamdar, Y. S. Kim, S.M. Pawar, J. H. Kim, H. Im, H. Kim, *J. Power Sources.*, 2011, **196**, 2393.
11 X. Sun, G. K. Wang, J.-Y. Hwang and J. Lian, *J. Mater. Chem.*, 2011, **21**, 16581.
12 S.-I. Kim, J.-S. Lee, H.-J. Ahn, H.-K. Song and J.-H. Jang, *ACS Appl. Mater. Interfaces*, 2013, **5**, 1596.
13 X. Y. Yan, X. L. Tong, J. Wang, C. W. Gong, M. G. Zhang and L. P. Liang, *Mater. Lett.*, 2013, **95**, 1.
14 B. Ren, M. Q. Fan, Q. Liu, J. Wang, D. L. Song and X. F. Bai, *Electrochim. Acta*, 2013, **92**, 197.
15 C. Z. Yuan, L. R. Hou, Y. L. Feng, S. L. Xiong and X. G. Zhang, *Electrochim. Acta*, 2013, **88**, 507.
16 Z. Y. Lu, Z. Chang, J. F. Liu and X. M. Sun, *Nano Res.*, 2011, **4**, 658.
17 20 M.-S. Wu,Y.-A. Huang and C.-H. Yang, *J. Electrochem. Soc.*, 2008, **155**, A798.
18 (a) D. F. Pickett and J. T. Maloy, *J. Electrochem. Soc.*, 1978, **125**, 1026; (b) G.-W. Yang, C.-L. Xu and H.-L. Li, *Chem. Commun.*, 2008, 6537.
19 Y.-M. Wang, D.-D. Zhao, Y.-Q. Zhao, C.-L. Xu and H.-L. Li, *RSC Advances*, 2012, **2**, 1074.
20 H. W. Wang, H. Yi, X. Chen and X. F. Wang, *Electrochim. Acta*, 2013, **105**, 353.
21 Y. Y. Xi, D. Li, A. B. Djurišić, M. H. Xie, K. Y. K. Man and W. K. Chan, *Electrochem. Solid-State Lett.*, 2008, **11**, D56.
22 D. Tench and L. F. Warren, *J. Electrochem. Soc.*, 1983. **130**, 869.
23 M.-S. Wu and C.-H. Yang, *Appl. Phys. Lett.*, 2007, **91**, 033109.
24 M.-S.Wu,Y.-A. Huang, C.-H.Yang and J.-J. Jow, *Int. J. Hydrogen. Energ.*, 2007, **32**, 4153.
25 W. Xing, S. Z. Qiao, X. Z. Wu, X. L. Gao, J. Zhou,S. P. Zhuo, S. B. Hartono and D. H.-Jurcakova, *J. Power Sources.*, 2011, **196**, 4123.
26 R. Farhi and G. Petot-ervas, *J. Phys. Colloques*, 1976, **37**, C7-438.
27 S. Takahashi, M. Oishi, E. Takeda, Y. Kubota, T. Kikuch and K. Furuya, *Biol. Trace Elem. Res.*, 1999, **69**, 161
28 M.-S. Wu and M.-J. Wang, *Chem. Commun.*, 2010, **46**, 6968.
29 Q. Lu, M. W. Lattanzi, Y. P. Chen, X. M. Kou, W. F. Li, X. Fan, K. M. Unruh, J. G. Chen and J. Q. Xiao, *Angew. Chem. Int. Ed.*, 2011, **50**, 6847.
30 Y. L. Wang, Y. Q. Zhao and C. L. Xu, *J. Solid State Electrochem.*, 2012, **16**, 829
31 X. H. Lu, T. Zhai, X. H. Zhang, Y. Q. Shen, L. Y. Yuan, B. Hu, L. Gong, J. Chen, Y. H. Gao, J. Zhou, Y. X. Tong and Z. L. Wang, *Adv. Mater.*, 2012, **24**, 938.
32 C. C. Hu, K. H. Chang and T. Y. Hsu, *J. Electrochem. Soc.*, 2008, **155**, F196.
33 C. Z. Yuan, X. G. Zhang, L. H. Su, B. Gao and L. F. Shen, *J. Mater. Chem.*, 2009, 19, 5772.
34 T. Y. Wei, C. H. Chen, H. C. Chien, S. Y. Lu and C. C. Hu, *Adv. Mater.*, 2010, **22**, 347.
35 X. M. Liu, Y. H. Zhang, X. G. Zhang and S. Y. Fu, *Electrochim. Acta*, 2004, **49**, 3137.
36 C. Bocca, A. Barbucci and G. Cerisola, *Int. J. Hydrogen Energ.*, 1998, **23**, 247.
37 K. Juodkazis, J. Juodkazytė, R. Vilkauskaitė and V. Jasulaitienė, *J. Solid State Electrochem.*, 2008, **12**, 1469.